Bull. Chem. Soc. Ethiop. **2023**, 37(1), 197-210.
DOI: https://dx.doi.org/10.4314/bcse.v37i1.16

ISSN 1011-3924
Printed in Ethiopia
Online ISSN 1726-801X

DECOLORIZATION OF REACTIVE AZO DYE BY FENTON AND PHOTO-FENTON PROCESSES IN AQUEOUS SOLUTION: THE INFLUENCE OF OPERATING CONDITIONS, KINETICS STUDY, AND PERFORMANCE COMPARISON

Gökçe Didar Değermenci*

Department of Environmental Engineering, Kastamonu University, 37150, Kastamonu, Turkey

(Received June 15, 2022; Revised September 14, 2022; Accepted September 14, 2022)

ABSTRACT. In this study, the effect of Fenton and photo-Fenton processes, which are advanced oxidation processes that use the hydroxyl radical for the decolorization of Novacron Black from aqueous solutions, on decolorization was investigated. Optimum levels of initial pH, temperature, hydrogen peroxide concentration, initial dyestuff concentration, and iron concentration were determined. Initial pH, Fe^{2+} concentration, temperature, and initial Novacron Black concentration are the most effective experimental parameters in the decolorization of Novacron Black with Fenton and photo-Fenton processes. While the Novacron Black concentration was 200 mg/L, the H_2O_2 concentration was 100 mg/L, the initial solution pH was 3, and the temperature was 20 °C, a decolorization efficiency of 82.1% was obtained in the Fenton process at a concentration of 5 mg/L Fe^{2+}, while in the photo-Fenton process at a 2 mg/L Fe^{2+} concentration, a 94.6% decolorization efficiency was obtained. Upon decolorization of Novacron Black, the photo-Fenton process had a higher removal efficiency than the Fenton process, even at low iron concentrations. From data obtained at various concentrations of initial Novacron Black, the non-linear method was used to determine the decolorization kinetics of Novacron Black. Finally, an economic analysis was carried out to compare the differences in operating costs between Fenton and photo-Fenton processes.

KEY WORDS: Advanced oxidation process, Decolorization, Fenton oxidation, Kinetic model, Photo-Fenton oxidation

INTRODUCTION

Even though water covers 74% of the surface of the earth, just 0.26% of it can be accessed. Water resources are rapidly contaminated by industries discharging their wastewater directly or without adequate treatment into these limited accessible water resources [1]. The textile industry's wastewater, which contains large amounts of synthetic dyestuffs, is also another significant contaminant source and a threat to aquatic ecosystems. While the annual production of synthetic dyes is around $7x10^5$ tons, it is estimated that around 50,000 tons of dye-containing wastewater is discharged into the receiving environment [2–4]. Discharging these dye-containing wastewaters to the receiving environment negatively affects photosynthesis by preventing light from passing through and decrease dissolved oxygen levels; they are also worrisome since they create toxic levels for flora and fauna even at low concentrations (> 1 ppm) [5, 6]. The textile industry employs a variety of dye classes (including dispersed, direct, complex, and reactive etc.) [7]. Reactive dyes are the most preferred dyes due to their easy covalent bonding to cotton fabric, high solubility, color variety, quick and chemical stability, and they are discharged into wastewater about 10% to 60% [8–10]. Studies have indicated that these dyes, which have an azo structure, have chromophore (C=C, N=N, C=O) and auxochrome (-OH, $-NH_2$, NR_2) functional groups, and these dyes pose a severe environmental threat due to their low biodegradability [11, 12]. Physical, chemical, and biological methods have been used for the removal of dyestuffs. For its simplicity and lack of formation of hazardous intermediates, adsorption is the method of choice; however, the adsorbent is reusable or regeneration, and this results in the creation of a secondary contaminant [13]. Coagulation, a widely used physical-chemical wastewater treatment process, has several advantages, such as low cost, convenience of use, and high efficiency, but it is

*Corresponding author. E-mail: gdegermenci@kastamonu.edu.tr ; gokcendidar@gmail.com

insufficient for the removal of stubborn dyes [14]. Although biological treatment is more environmentally friendly, sustainable, safe, and cheaper compared to other methods, some dyes and components in the dyeing process are toxic, resistant to biodegradation and require larger areas and longer retention times [15, 16]. Advanced oxidation methods that generate hydroxyl radicals are widely employed to break down and mineralize stubborn toxic compounds [17]. Fenton, photo-Fenton, electro-Fenton, ozonation at high pH, and electrochemical processes are among the most utilized in wastewater treatment.

The systems in which Fe^{2+} is utilized as a catalyst and H_2O_2 is used as an oxidant in an acidic environment to oxidize organic and inorganic contaminants are called the Fenton process (Eq. 1 and 2) [18]. Since the reduction of Fe^{3+} to Fe^{2+} in the presence of H_2O_2 is limited, this cycle is interrupted and Fe^{3+} accumulates instead, which reduces catalytic activity [19].

$$Fe^{2+} + H_2O_2 \rightarrow Fe^{3+} + {}^{\bullet}OH + OH^{-} \quad (1)$$

$$Fe^{3+} + H_2O_2 \rightarrow Fe^{2+} + {}^{\bullet}HO_2 + H^{+} \quad (2)$$

There are numerous advantages to the Fenton process, including low cost, fast reaction time, ease of application, and control [20]. However, there are disadvantages such as excessive chemical consumption, difficulty in separating solids from liquids in treated wastewater, and sludge disposal [21]. Since the regeneration of Fe^{2+} through the reaction of Fe^{3+} with H_2O_2 is limited in the Fenton process, this process determines the reaction rate (Eq. 2). To speed up the regeneration of Fe^{2+} and restart the regular Fenton reaction cycle, the Fenton process is supported by UV irradiation and is referred to as photo-Fenton [22]. The primary goal of the photo-Fenton process is to use the energy provided by UV irradiation to speed up the reduction of Fe^{3+} to Fe^{2+} [23]. Under UV irradiation, Fe^{2+} is regenerated, allowing H_2O_2 to decompose, and additional hydroxyl radicals, which degrade organic contaminants, are generated (Eq. 3). In addition, direct photolysis of H_2O_2 also generates hydroxyl radicals that can be employed to degrade organic contaminants (Eq. 4), increasing the oxidation efficiency [19, 24].

$$Fe^{3+} + H_2O \xrightarrow{hV} Fe^{2+} + {}^{\bullet}OH + H^{+} \quad (3)$$

$$H_2O_2 \xrightarrow{hV} 2\,{}^{\bullet}OH \quad (4)$$

The Novacron Black (NB) used in this study is a mixture of Reactive Black 39 and Reactive Brown 11 according to the material safety data sheet (MSDS) obtained from the importer company. It may cause an allergic skin reaction and serious eye irritation. Since the biodegradability of synthetic wastewater prepared from this dyestuff is very low, its decolorization was investigated using Fenton and photo-Fenton processes. Optimum conditions on NB decolorization were determined by investigating the effects of various operating parameters such as H_2O_2, Fe^{2+}, initial NB concentration, initial pH value and temperature. By using the experimental data obtained from these two processes, their compatibility with some kinetic models was examined.

EXPERIMENTAL

Chemicals

A textile production company in Bursa/Turkey provided the NB dye used in this study's synthetic samples. Hydrogen peroxide (H_2O_2, 30%), sulfuric acid (H_2SO_4, 95%), ferrous sulfate ($FeSO_4.7H_2O$, 99.5%) and sodium hydroxide (NaOH, >99%) were purchased from Merck. All the prepared solutions were made with deionized water. All the chemicals were used without additional purification.

Fenton and photo-Fenton processes

During the Fenton and photo-Fenton process experiments, a 500 mL double-walled glass reactor was used. Both reactors were operated in batch mode and mixed at 500 rpm using a magnetic stirrer (IKA, RCT basic) to ensure homogeneity. The light source for the photo-Fenton process was a low-pressure mercury vapor lamp (LightTech, GPH 212T5/L4, 10W, 254 nm). The light source was housed in a quartz sleeve that aligns coaxially with the reactor. The temperature was kept constant at the desired value by using a temperature-controlled heated-cooled circulator (LABO, C200-H13). pH values were measured using WTW brand Multi 3620 IDS model pH meter. Before it was put into the reactor, the light source was operated for around 15 min to achieve a steady light intensity. In addition, the reactor's exterior was wrapped in aluminum foil to prevent the light source from being lost. The photon flux entering the solution was measured as 2.291 μEinstein/s by the KI/KIO_3 actinometer method [25]. The effects of solution's initial pH (2–6), Fe^{2+} concentration (1–10 mg/L), H_2O_2 concentration (17–100 mg/L), initial dye concentration (100 – 400 mg/L) and temperature (10–40 °C) parameters on contaminant removal were investigated in the removal of synthetic dye solution containing NB by Fenton and photo-Fenton processes. Each experiment had a reaction time of 60 min, and samples were collected and analyzed at specified intervals. A 0.2 M solution of H_2SO_4 or NaOH was used to adjust the initial pH values.

Analytical methods

NB concentrations were determined by measuring the absorbance values with a calibration curve prepared at the maximum wavelength (610 nm) using a UV-Vis spectrophotometer (Hach Lange, DR6000) immediately after the samples were taken during the experiments.

$$Percentage\,of\ decolorization = \left(1 - C/C_0\right) \times 100 \tag{5}$$

Here, C_0 is the initial NB concentration, and C is the NB concentration at any given time.

Kinetic modelling

The NB degradation was modeled using pseudo-first-order (Eq. 6), pseudo-second-order (Eq. 7), and Behnajady-Modirshahla-Ghanbery (BMG) (Eq. 8) kinetic models. The non-linear method and the Solver plug-in in Microsoft Excel were used to derive the coefficients of the models that were used.

$$\ln\left(C/C_0\right) = -k_1 \times t \tag{6}$$

$$1/C - 1/C_0 = k_2 \times t \tag{7}$$

$$C/C_0 = 1 - t/\left(m + bt\right) \tag{8}$$

Here C (mg/L) and C_0 (mg/L) are the NB concentration at any given time, t (min) and at initial, respectively, k_1 (min^{-1}) and k_2 (L mg^{-1} min^{-1}) represent the pseudo-first-order and pseudo-second-order rate constants, respectively, b and m (min) represent the theoretical oxidation capacity and reaction kinetics for the BMG model, respectively. The higher the 1/m value, the faster the dyestuff's initial degradation rate. Likewise, the 1/b value represents the maximum theoretical decay fraction.

RESULTS AND DISCUSSION

Decolorization of NB in deionized water

The effects of H_2O_2, Fe^{2+}, and UV alone, and the effects of UV/Fe^{2+}, UV/H_2O_2, Fenton, and photo-Fenton processes, were investigated for the decolorization of NB employing advanced oxidation processes (Figure 1). At pH 3, both Fe^{2+} and H_2O_2 remained ineffective in degrading NB on their own. Decolorization efficiency under UV irradiation was 7.7% after 60 min, but with Fe^{2+} added (UV/Fe^{2+}) and H_2O_2 added (UV/H_2O_2), it rose to 14.3% and to 51.4%, respectively. While the decolorization efficiency was 94.3% in the process (Fenton) where Fe^{2+} and H_2O_2 were used together, it was 96.6% in the photo-Fenton process (UV/Fe^{2+}/H_2O_2). NB dye decolorization with the Fenton process was approximately 80% in 7.5 min, but the photo-Fenton process achieved a similar level of decolorization efficiency in approximately 5 min, as shown in Figure 1. Under these experimental conditions, it can be concluded that the Fenton and photo-Fenton processes are far more effective than other processes in the decolorization of NB. The high decolorization efficiency of Fenton and photo-Fenton processes can be attributed to the generation of large amounts of hydroxyl radicals.

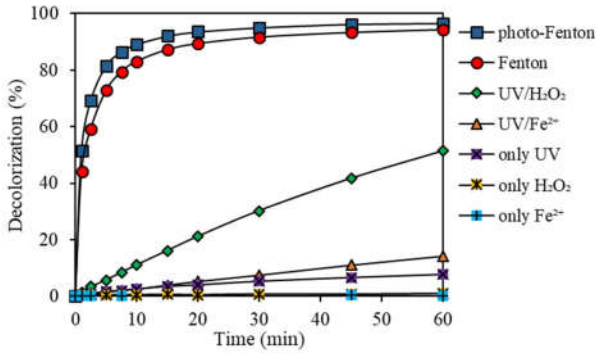

Figure 1. Decolorization of NB with different methods (experimental conditions: NB = 200 mg/L, T = 20 °C, Fe^{2+} = 5 mg/L, H_2O_2 = 100 mg/L, initial pH = 3).

Effect of initial solution pH on the decolorization

A key operating parameter that affects removal of contaminants in Fenton and photo-Fenton processes is the initial pH value. The generation of hydroxyl radicals in these processes is highly sensitive to the pH of the solution [26]. The Fenton oxidation process generates hydroxyl radicals because of the reaction of Fe^{2+} ion with H_2O_2 under acidic conditions. Experiments were conducted under acidic conditions at different pH values to identify the optimum pH value for both processes. Temperature, H_2O_2, Fe^{2+}, and NB concentration were 20 °C, 100 mg/L, 5 mg/L, and 200 mg/L, respectively, in the experiments. Decolorization efficiency results are shown in Figure 2 as an outcome of the experiments. The pH of the solution had a significant effect on the decolorization of NB in both processes. For all pH values, the photo-Fenton process had a higher decolorization efficiency than the Fenton process. Maximum decolorization efficiency was achieved at pH 3 in Fenton and photo-Fenton processes. The decolorization efficiency of the NB dye at pH 3 was around 94.3% at the end of the 60 minutes in the Fenton process, while it was 96.6% in the photo-Fenton process. NB decolorization decreased in both processes at pH 2. After 60 min, the Fenton process's decolorization efficiency was 86.3%, whereas the photo-Fenton

process's was 96.1%. The decrease in efficiency at pH 2 in both processes can be attributed to the generation of hydronium ions (Eq. 9) and the reaction of some of the hydroxyl radicals with the high amount of H^+ ions (Eq. 10) [17, 27]. A decolorization efficiency of 86.8% was achieved at pH 4 after 60 min in the Fenton process, but this reduced to 53.8% at pH 5 and to 11.3% at pH 6. Decolorization efficiency at pH 4 was 96.0% after 60 min in the photo-Fenton process, which reduced to 91.9% at pH 5 and to 85.7% at pH 6. The formation of Fe^{2+}/Fe^{3+} hydroxide complexes increases in both processes as the pH of the solution rises, suppressing the Fe^{2+} catalyst and reducing the amount of hydroxyl radical generated [27]. Therefore, the decolorization of NB is reduced in both processes. However, due to UV irradiation, Fe^{3+} is reduced to Fe^{2+} in the photo-Fenton process, which leads to the generation of more radicals than the Fenton process [28]. The optimum initial pH value for Fenton and the photo-Fenton process was chosen as pH 3, which is the value at which the maximum decolorization efficiency occurs.

$$H_2O_2 + H^+ \rightarrow H_3O_2^+ \tag{9}$$

$$^{\bullet}OH + H^+ + e^- \rightarrow H_2O \tag{10}$$

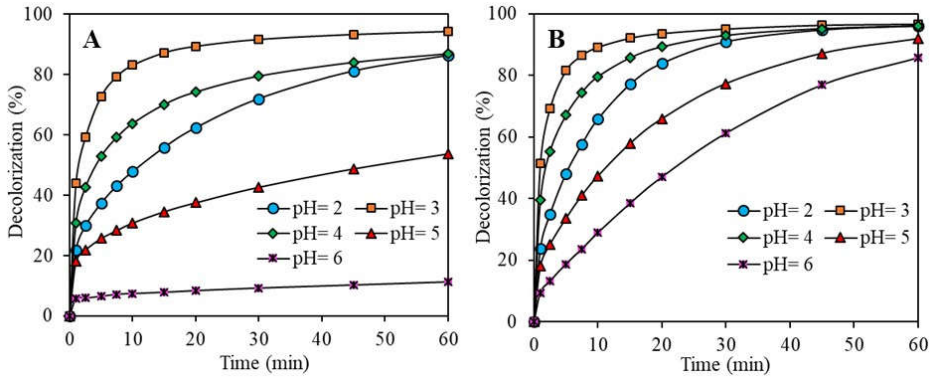

Figure 2. The decolorization of NB for Fenton (A) and photo-Fenton (B) at different initial solution pH (experimental conditions: NB = 200 mg/L, T = 20 °C, Fe^{2+} = 5 mg/L, H_2O_2 = 100 mg/L).

Effect of Fe^{2+} dosage on the decolorization

As a catalyst in the Fenton and photo-Fenton process, Fe^{2+} is an important parameter that affects the removal of organic contaminants. In this experimental series, the effect of Fe^{2+} ion concentration on the decolorization of NB was investigated for 1, 2, 5 and 10 mg/L. The parameters were set as initial NB concentration 200 mg/L, H_2O_2 concentration 100 mg/L, initial solution pH 3 and temperature 20 °C. Figure 3 shows the effect of Fe^{2+} ions on NB decolorization. The decolorization efficiency of Fe^{2+} concentration at 1 mg/L and 60 min reaction time is 59.5% in the Fenton process and 87.9% in the photo-Fenton process. By increasing the Fe^{2+} concentration to 2 mg/L, the decolorization efficiency reached 82.1% in the Fenton process and 94.6% in the photo-Fenton process in the 60 min of reaction time. The decolorization efficiency of Fenton and photo-Fenton processes was not significantly changed by increasing the Fe^{2+} concentration to 5 and 10 mg/L for 60 min of reaction time. It was found that the photo-Fenton process, rather than the Fenton process, had a higher removal efficiency even at low iron concentrations. As a result, similar decolorization efficiency with the Fenton process can be achieved using less Fe^{2+} in the

photo-Fenton process. This can be attributed to the increase in the formation of hydroxyl radical species responsible for the decolorization of NB, namely the reduction of Fe^{3+} to Fe^{2+}. Generally, since hydroxyl radical generation in Fenton processes is proportional to Fe^{2+} concentrations, decolorization efficiency is lower at low Fe^{2+} concentrations. Lower decolorization efficiency can be observed at high concentrations, due to hydroxyl radical scavenging [29]. The optimum concentration of Fe^{2+} was determined to be 5 mg/L, considering both processes.

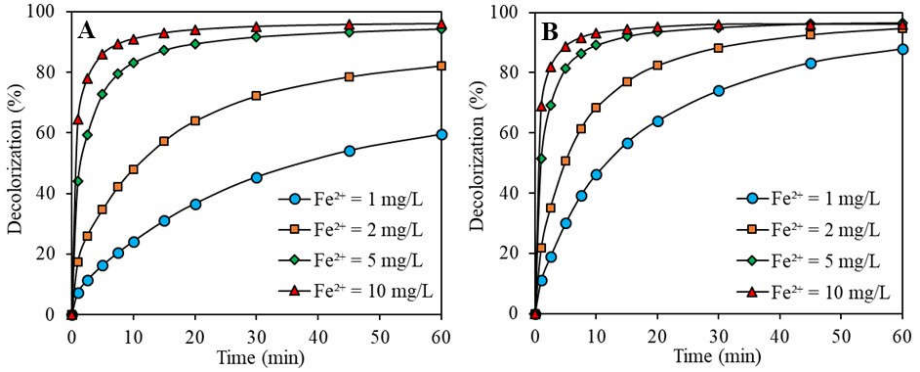

Figure 3. The decolorization of NB in Fenton (A) and photo-Fenton (B) systems at different Fe^{2+} dosage. (Experimental conditions: NB = 200 mg/L, T = 20 °C, H_2O_2 = 100 mg/L, initial pH = 3).

Effect of H_2O_2 dosage on the decolorization

The oxidation of organic contaminants is related to the amount of oxidant added to the reaction medium (solution). H_2O_2 is used as the oxidant in the Fenton and photo-Fenton process. The main operating cost is H_2O_2 in the Fenton process, and H_2O_2 and UV light source in the photo-Fenton process. In general, the removal of the contaminant rises when the Fenton process contains more H_2O_2. Therefore, the effect of different hydrogen peroxide concentrations (17, 34, 50 and 100 mg/L) was optimized by keeping other experimental parameters (initial pH value, initial contaminant concentration, Fe^{2+} dosage and temperature) constant, and the experimental results were shown in Figure 4. When the decolorization efficiencies of NB in Fenton and photo-Fenton processes were compared, the NB decolorization efficiency in the first 30 minutes increased from 64.6% to 91.7% in the Fenton process, and from 65.1% to 95.1% in the photo-Fenton process. Similar decolorization efficiency with the Fenton process can be achieved by using less H_2O_2 in the photo-Fenton process. This is due to the effectiveness of ultraviolet rays. Researchers have stated that in the presence of excess hydrogen peroxide, possible secondary reactions occur between H_2O_2 and the hydroxyl radical ($^{\bullet}OH$), resulting in a decrease in the activity of the hydroxyl radical (Eq. 11 and 12) [30, 31]. This causes the removal efficiency of contaminants to decrease. For example, it was stated that using the photo-Fenton process to remove ciprofloxacin hydrochloride, the decolorization efficiency rose from 65% to 98% after 60 min, with the H_2O_2 concentration rising from 0.25 mmol/L to 5 mmol/L. However, it was reported that further increasing the concentration of H_2O_2 did not boost the removal efficiency and even decreased slightly [32]. It should also be noted that excessive use of H_2O_2 increases the cost of removal. The 50 mg/L H_2O_2 concentration was determined to be optimum for both processes considering the experimental conditions and the H_2O_2 cost.

$$H_2O_2 + {}^{\bullet}OH \rightarrow H_2O + {}^{\bullet}HO_2 \quad (11)$$

$${}^{\bullet}OH + {}^{\bullet}OH \rightarrow H_2O_2 \quad (12)$$

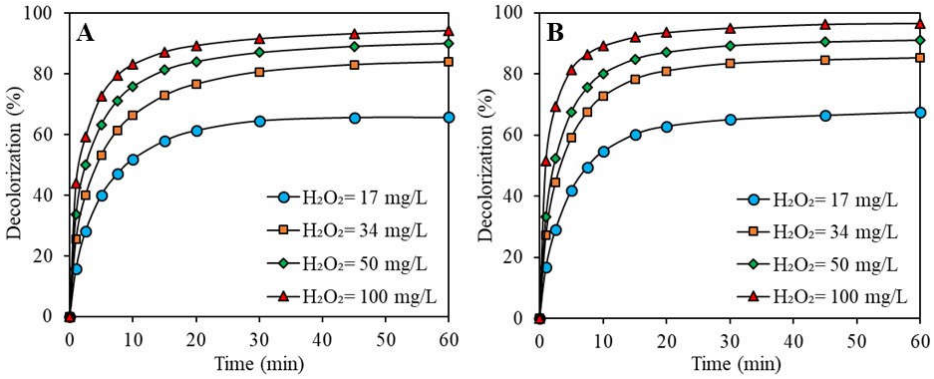

Figure 4. The decolorization of NB in Fenton (A) and photo-Fenton (B) systems at different H_2O_2 dosage. (Experimental conditions: NB = 200 mg/L, T = 20 °C, Fe^{2+} = 5 mg/L, Initial pH = 3).

Effect of initial NB concentration

Color levels of wastewater generated in industries can have different values depending on the production process and the amount of water used. Therefore, the removal of wastewater with various organic loads can exhibit variations. In Fenton and photo-Fenton processes, the effect of initial contaminant concentration on decolorization was therefore investigated. To determine the effect of the initial NB concentration on the decolorization efficiency, experiments were conducted at various NB concentrations (100-400 mg/L). Figure 5 illustrates the results obtained.

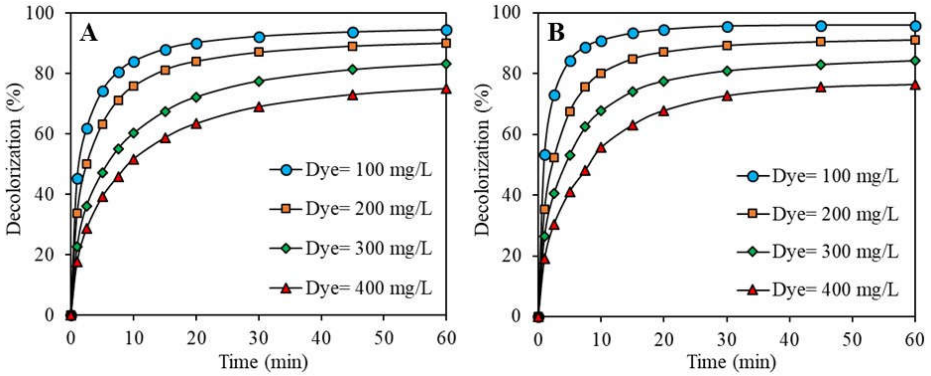

Figure 5. The decolorization of NB in Fenton (A) and photo-Fenton (B) systems at different initial NB concentrations. (Experimental conditions: H_2O_2 = 50 mg/L, T = 20 °C, Fe^{2+} = 5 mg/L, initial pH = 3).

Both processes saw a decline in decolorization efficiency as the initial dye concentration increased. When the dyestuff concentration was increased from 100 mg/L to 400 mg/L in the Fenton process, decolorization efficiency reduced from approximately 95% to 75% in a reaction time of 60 min. In the photo-Fenton process, it decreased from approximately 96% to 77%. Decolorization efficiency is always lower when the NB concentration in both processes increase since the hydroxyl radical concentration generated is not affected by this increase. Similarly, in a study in which methylene blue removal was performed, it was stated that by increasing the initial dye concentration from 10 mg/L to 50 mg/L, the decolorization efficiency decreased from 95.6% to 84.2% after 60 min [29]. In another study, it was indicated that at high dye concentrations, UV irradiation was adsorbed by dye molecules instead of H_2O_2, limiting the generation of hydroxyl radicals and reducing the decolorization of the dyestuff [33]. It was also suggested that photons entering the solution at high dye concentrations in the photo-Fenton process limit penetration and, as a result, can decrease the hydroxyl radical concentration [34].

Effect of temperature

Temperature rise is an important factor in the Fenton and photo-Fenton process. Figure 6 shows the effect of NB dye on decolorization efficiency at different temperatures (10, 20, 30 and 40 °C) in Fenton and photo-Fenton processes. Experiments were conducted under conditions optimized for 300 mg/L NB dye. Temperature rise has a significant effect on the removal of NB dye, as seen in Figure 6. With the temperature rise, the decolorization efficiency of NB dye increased from 45.3% to 85.1% in the Fenton process and from 60.3% to 85.4% in the photo-Fenton process after 15 min. The decolorization efficiency of NB dye in the Fenton process increased from 69.3% to 86.9% and from 80.67% to 86.9% in the photo-Fenton process when the reaction time was 60 min. Temperature rise accelerates the reaction between H_2O_2 and Fe^{2+} and leads to an increase in the hydroxyl radical generation rate for both processes [35]. Thus, the rate of decolorization increases because of an increase in the generation of hydroxyl radicals. The results of the kinetic analysis for both processes have confirmed that the kinetic coefficients increase with temperature rise. When the effect of temperature is examined in terms of removal rates, the photo-Fenton process is 1.71 times more effective than the Fenton process at 10 °C and 1.44 times more effective at 20 °C. At 30 °C and 40 °C, the decolorization rates are almost the same for both processes. It is important to note, however, that the removal efficiency of contaminants may decrease when the temperature exceeds the optimum value. Decomposition of H_2O_2 into H_2O and O_2 may be a viable reason for this decrease in the number of hydroxyl radicals generated during this process [35].

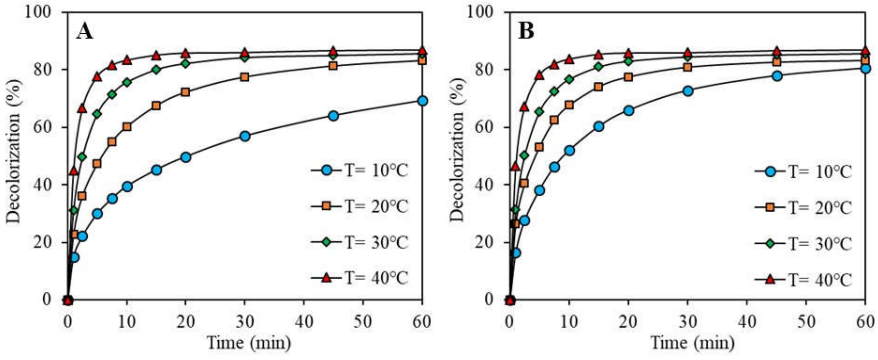

Figure 6. The decolorization of NB in Fenton (A) and photo-Fenton (B) systems at different temperatures. (Experimental conditions: NB = 300 mg/L, H_2O_2 = 50 mg/L, Fe^{2+} = 5 mg/L, initial pH = 3).

Decolorization kinetics

For various initial dyestuff concentrations, kinetic calculations were performed after the optimization research. Pseudo-first-order (Eq. 6), pseudo-second-order (Eq. 7), and Behnajady-Modirshahla-Ghanbery (BMG) (Eq. 8) [36–38] kinetic models were used to test the decolorization kinetics of NB dye with Fenton and photo-Fenton processes. The linear forms of these kinetic models have been reported in several studies as causing incorrect results and wrong conclusions [39, 40]. Furthermore, it has been shown in the literature that nonlinear forms deliver better results than linear forms when it comes to fitting experimental data [41]. Thus, the kinetic coefficients were determined using the non-linear method with the help of Microsoft Excel Solver plug-in. The non-linear plots and parameters were shown in Table 1 and Figure 7. The kinetic data obtained from the decolorization of NB showed that the coefficients of determination (R^2) of the BMG kinetic model were larger (BMG > pseudo-second-order > pseudo-first-order) than those of the pseudo-first-order and pseudo-second-order kinetic models. According to these results, the BMG kinetic model is much more compatible with the experimental data to describe the decolorization of NB. This kinetic model has also been applied in different studies to describe the dye and pesticide removal kinetics with the Fenton process [17, 42].

Table 1. The calculated parameters of the kinetic models used in the study.

Type of process	Experimental conditions					Pseudo-first-order		Pseudo-second-order		BMG		
	pH	H_2O_2 (mg/L)	Fe^{2+} (mg/L)	T (°C)	C_0 (mg/L)	k_1	R^2	k_2	R^2	b	m	R^2
Fenton	3	50	5	20	100	0.2570	0.8972	0.0062	0.9890	1.047	1.343	0.9974
	3	50	5	20	200	0.1395	0.8794	0.0017	0.9815	1.081	2.310	0.9975
	3	50	5	20	300	0.0593	0.8588	0.0005	0.9699	1.145	4.921	0.9942
	3	50	5	20	400	0.0356	0.8336	0.0002	0.9508	1.243	6.957	0.9956
photo-Fenton	3	50	5	20	100	0.5217	0.9426	0.0107	0.9979	1.019	0.864	0.9997
	3	50	5	20	200	0.1802	0.9089	0.0021	0.9911	1.053	2.055	0.9993
	3	50	5	20	300	0.0851	0.8443	0.0007	0.9674	1.133	3.463	0.9971
	3	50	5	20	400	0.0435	0.8319	0.0003	0.9561	1.204	6.085	0.9954

Operational cost analysis

The economic criteria between the two processes were taken into consideration to decide the operating conditions for the decolorization of NB with the Fenton and photo-Fenton processes. The photo-Fenton process has a higher operational cost because it also uses a UV light source in addition to the Fenton process. Photo-Fenton processes, on the other hand, can achieve the same decolorization efficiencies as Fenton processes at lower Fe^{2+} dosages. As a result, when operational costs at various Fe^{2+} dosages were calculated for both processes, the differences between them were calculated (temperature, mixing speed, H_2O_2 dosage and initial pH are fixed for both processes, these parameters were not included in the operating calculation). While $FeSO_4.7H_2O$ was taken into consideration while calculating the cost of the Fenton process, the amount of $FeSO_4.7H_2O$ and the electrical energy consumed by UV were taken into consideration in the photo-Fenton process. Energy costs were calculated at €71/MWh, and the $FeSO_4.7H_2O$ cost was calculated at €9.5/kg [43]. The photo-Fenton process's lowest operational costs were achieved at a Fe^{2+} concentration of 2 mg/L for a UV lamp power of 10 W, a reactor volume of 0.5 L, and decolorization efficiencies of 60% and 90%. Similar decolorization efficiencies were achieved at 5 mg/L Fe^{2+} concentration in the Fenton process, and the photo-Fenton process cost was calculated to be equal to that of the Fenton process. Since less Fe^{2+} is employed in the photo-Fenton process for the same decolorization efficiencies, the lower cost of disposal of the generated iron sludge should be considered an advantage of this process.

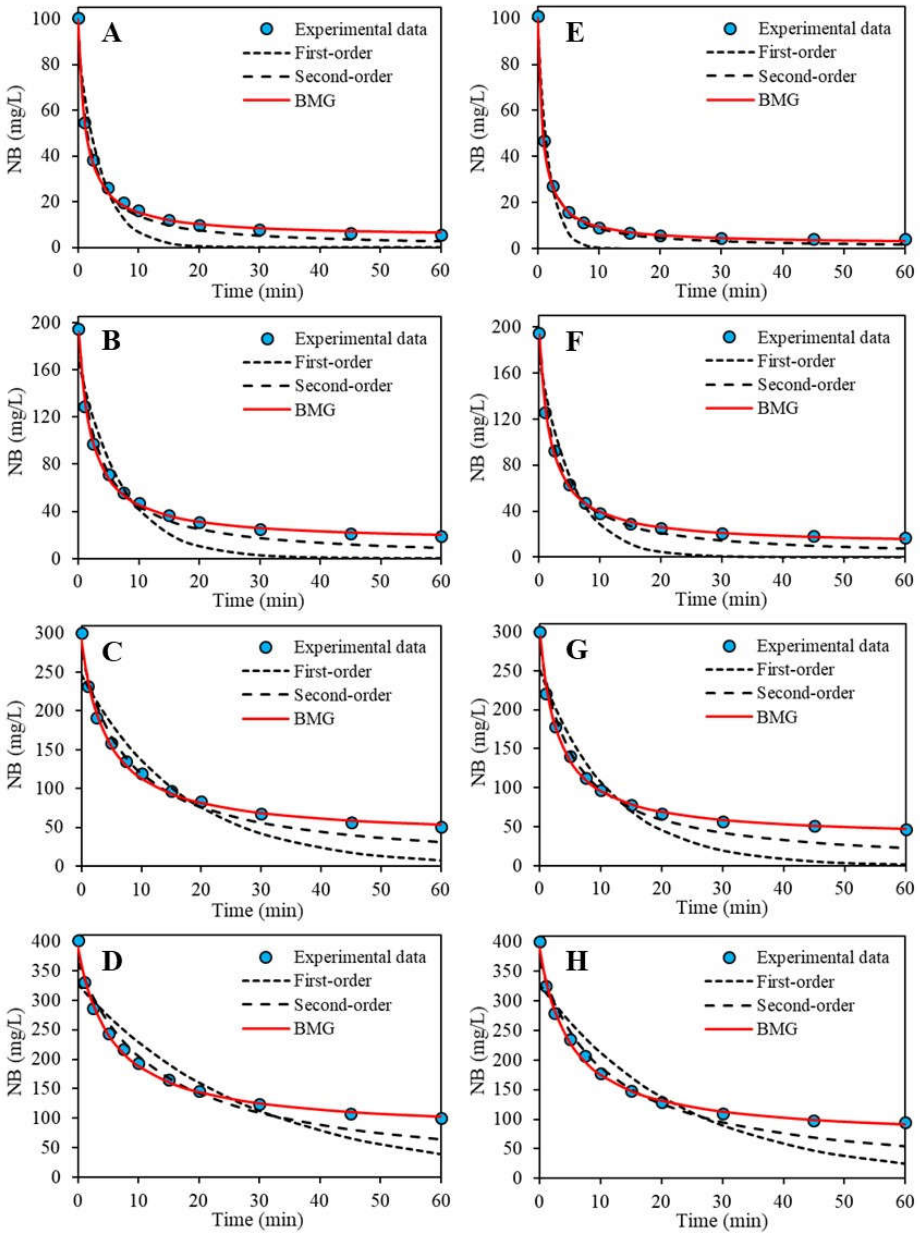

Figure 7. Experimental data, first order kinetic model, second order kinetic model, and BMG kinetic model for the decolorization of NB in Fenton process (A, B, C, D) and photo-Fenton process (E, F, G, H). (Experimental conditions: H_2O_2 = 50 mg/L, T = 20 °C, Fe^{2+} = 5 mg/L, initial pH = 3).

CONCLUSION

Fenton and photo-Fenton oxidation decolorization of NB, a model contaminant found in textile wastewater, has been successfully carried out. Initial pH, Fe^{2+} concentration, temperature, and initial NB concentration are the most effective experimental parameters in the decolorization of NB with Fenton and photo-Fenton processes. The Fenton process was shown to be significantly affected by pH changes compared to the photo-Fenton process. The increase in the pH of the solution in the Fenton process leads to the suppression of the Fe^{2+} catalyst, which reduces the amount of hydroxyl radical produced, thus reducing the decolorization of NB. However, in the photo-Fenton process, Fe^{3+} is reduced to Fe^{2+} due to UV irradiation, leading to higher decolorization efficiencies compared to the Fenton process. On the decolorization of the NB, it was found that the photo-Fenton process, rather than the Fenton process, had a higher removal efficiency even at low iron concentrations. Thus, it can be concluded that using less Fe^{2+} in the photo-Fenton process can achieve a similar level of decolorization efficiency as can be achieved with the Fenton process. For 10 °C, the photo-Fenton process is 1.71 times more effective than the Fenton process in terms of removal rates, and for 20 °C, it is 1.44 times more effective than the Fenton process. At 30 °C and 40 °C, the decolorization rates are almost the same for both processes. To explain the experimental results, the BMG kinetic model of the highest coefficient of determination was calculated using the non-linear method. For the decolorization costs calculated based on NB's 60% and 90% decolorization efficiencies, the photo-Fenton process yielded the lowest operational cost at 2 mg/L Fe^{2+} concentration, while the Fenton process achieved similar decolorization efficiency at 5 mg/L Fe^{2+}.

ACKNOWLEDGMENT

We would like to thank Nejdet Değermenci, Esma Sebile Eroğlu, Tuba Sağlık, and Melike Celepverdi for their contributions to several of the analyzes.

REFERENCES

1. Tariq, M.; Muhammad, M.; Khan, J.; Raziq, A.; Uddin, M.K.; Niaz, A.; Ahmed, S.S.; Rahim, A. Removal of Rhodamine B dye from aqueous solutions using photo-Fenton processes and novel Ni-Cu@MWCNTs photocatalyst. *J. Mol. Liq.* **2020**, 312, 113399.
2. Lee, Y.C.; Amini, M.H.M.; Sulaiman, N.S.; Mazlan, M.; Boon, J.G. Batch adsorption and isothermic studies of malachite green dye adsorption using leucaena leucocephala biomass as potential adsorbent in water treatment. *Songklanakarin J. Sci. Technol.* **2018**, 40, 563–569.
3. Fernades Rêgo, F.E.; Sales Solano, A.M.; Da Costa Soares, I.C.; Da Silva, D.R.; Martinez Huitle, C.A.; Panizza, M. Application of electro-Fenton process as alternative for degradation of Novacron Blue dye. *J. Environ. Chem. Eng.* **2014**, 2, 875–880.
4. Singh, J.; Sharma, S.; Aanchal; Basu, S. Synthesis of Fe_2O_3/TiO_2 monoliths for the enhanced degradation of industrial dye and pesticide via photo-Fenton catalysis. *J. Photochem. Photobiol. A Chem.* **2019**, 376, 32–42.
5. Semião, M.A.; Haminiuk, C.W.I.; Maciel, G.M. Residual diatomaceous earth as a potential and cost effective biosorbent of the azo textile dye Reactive Blue 160. *J. Environ. Chem. Eng.* **2020**, 8, 103617.
6. Miyashiro, C.S.; Mateus, G.A.P.; dos Santos, T.R.T.; Paludo, M.P.; Bergamasco, R.; Fagundes-Klen, M.R. Synthesis and performance evaluation of a magnetic biocoagulant in the removal of reactive black 5 dye in aqueous medium. *Mater. Sci. Eng. C.* **2021**, 119, 111523.

7. Criado, S.P.; Gonçalves, M.J.; Ballod Tavares, L.B.; Bertoli, S.L. Optimization of electrocoagulation process for disperse and reactive dyes using the response surface method with reuse application. *J. Clean. Prod.* **2020**, 275, 122690.
8. Tanzifi, M.; Tavakkoli Yaraki, M.; Beiramzadeh, Z.; Heidarpoor Saremi, L.; Najafifard, M.; Moradi, H.; Mansouri, M.; Karami, M.; Bazgir, H. Carboxymethyl cellulose improved adsorption capacity of polypyrrole/CMC composite nanoparticles for removal of reactive dyes: Experimental optimization and DFT calculation. *Chemosphere.* **2020**, 255, 127052.
9. Nga, N.K.; Thuy Chau, N.T.; Viet, P.H. Preparation and characterization of a chitosan/MgO composite for the effective removal of reactive blue 19 dye from aqueous solution. *J. Sci. Adv. Mater. Devices.* **2020**, 5, 65–72.
10. Gautam, D.; Saya, L.; Hooda, S. Fe_3O_4 loaded chitin – A promising nano adsorbent for Reactive Blue 13 dye. *Environ. Adv.* **2020**, 2, 100014.
11. Jaafari, J.; Barzanouni, H.; Mazloomi, S.; Amir Abadi Farahani, N.; Sharafi, K.; Soleimani, P.; Haghighat, G.A. Effective adsorptive removal of reactive dyes by magnetic chitosan nanoparticles: Kinetic, isothermal studies and response surface methodology. *Int. J. Biol. Macromol.* **2020**, 164, 344–355.
12. Jawad, A.H.; Mubarak, N.S.A.; Abdulhameed, A.S. Tunable Schiff's base-cross-linked chitosan composite for the removal of reactive red 120 dye: Adsorption and mechanism study. *Int. J. Biol. Macromol.* **2020**, 142, 732–741.
13. Değermenci, G.D.; Değermenci, N.; Ayvaoğlu, V.; Durmaz, E.; Çakır, D.; Akan, E. Adsorption of reactive dyes on lignocellulosic waste; characterization, equilibrium, kinetic and thermodynamic studies. *J. Clean. Prod.* **2019**, 225, 1220–1229.
14. Mcyotto, F.; Wei, Q.; Macharia, D.K.; Huang, M.; Shen, C.; Chow, C.W.K. Effect of dye structure on color removal efficiency by coagulation. *Chem. Eng. J.* **2021**, 405, 126674.
15. Saleh, M.; Bilici, Z.; Kaya, M.; Yalvac, M.; Arslan, H.; Yatmaz Cengiz, H.; Dizge, N. The use of basalt powder as a natural heterogeneous catalyst in the Fenton and Photo-Fenton oxidation of cationic dyes. *Adv. Powder Technol.* **2021**, 32, 1264–1275.
16. Ravadelli, M.; da Costa, R.E.; Lobo-Recio, M.A.; Akaboci, T.R.V.; Bassin, J.P.; Lapolli, F.R.; Belli, T.J. Anoxic/oxic membrane bioreactor assisted by electrocoagulation for the treatment of azo-dye containing wastewater. *J. Environ. Chem. Eng.* **2021**, 9, 105286.
17. Değermenci, N.; Değermenci, G.D.; Ulu, H.B. Decolorization of reactive azo dye from aqueous solutions with Fenton oxidation process: effect of system parameters and kinetic study. *Desalin. Water Treat.* **2019**, 169, 363–371.
18. Austen, V.; Suyitno, C.; Gah, T.Y.P.R.; Sugiarta, P.; Santoso, S.P.; Edi Soetaredjo, F.; Foe, K.; Angkawidjaja, A.E.; Ju, Y.-H.; Ismadji, S. Fenton reagent for organic compound removal in wastewater. *J. Indones. Chem. Soc.* **2020**, 3, 1–16.
19. Zhang, M.H.; Dong, H.; Zhao, L.; Wang, D.X.; Meng, D. A review on Fenton process for organic wastewater treatment based on optimization perspective. *Sci. Total Environ.* **2019**, 670, 110–121.
20. Jia, N.; Yun, L.; Huang, J.; Chen, H.; Shen, C.; Wen, Y. A sandwich model of Cr(VI) adsorption and detoxification by Fenton modified chitosan. *Water Environ. Res.* **2021**, 93, 645–651.
21. Ribeiro, J.P.; Marques, C.C.; Portugal, I.; Nunes, M.I. Fenton processes for AOX removal from a kraft pulp bleaching industrial wastewater: Optimisation of operating conditions and cost assessment. *J. Environ. Chem. Eng.* **2020**, 8, 104032.
22. Will, I.B.S.; Moraes, J.E.F.; Teixeira, A.C.S.C.; Guardani, R.; Nascimento, C.A.O. Photo-Fenton degradation of wastewater containing organic compounds in solar reactors. *Sep. Purif. Technol.* **2004**, 34, 51–57.
23. Kalal, S.; Singh Chauhan, N.P.; Ameta, N.; Ameta, R.; Kumar, S.; Punjabi, P.B. Role of copper pyrovanadate as heterogeneous photo-Fenton like catalyst for the degradation of neutral red and azure-B: An eco-friendly approach. *Korean J. Chem. Eng.* **2014**, 31, 2183–

2191.
24. Maroudas, A.; Pandis, P.K.; Chatzopoulou, A.; Davellas, L.R.; Sourkouni, G.; Argirusis, C. Synergetic decolorization of azo dyes using ultrasounds, photocatalysis and photo-fenton reaction. *Ultrason. Sonochem.* **2021**, 71, 105367.
25. Bolton, J.R.; Stefan, M.I.; Shaw, P.S.; Lykke, K.R. Determination of the quantum yields of the potassium ferrioxalate and potassium iodide-iodate actinometers and a method for the calibration of radiometer detectors. *J. Photochem. Photobiol. A Chem.* **2011**, 222, 166–169.
26. Santana, R.M.D.R.; Napoleão, D.C.; Duarte, M.M.M.B. Treatment of textile matrices using Fenton processes: Influence of operational parameters on degradation kinetics, ecotoxicity evaluation and application in real wastewater. *J. Environ. Sci. Heal. - Part A Toxic/Hazard. Subst. Environ. Eng.* **2021**, 56, 1165–1178.
27. Hassan, A.K.; Rahman, M.M.; Chattopadhay, G.; Naidu, R. Kinetic of the degradation of sulfanilic acid azochromotrop (SPADNS) by Fenton process coupled with ultrasonic irradiation or L-cysteine acceleration. *Environ. Technol. Innov.* **2019**, 15, 100380.
28. Moradi, M.; Elahinia, A.; Vasseghian, Y.; Dragoi, E.N.; Omidi, F.; Mousavi Khaneghah, A. A review on pollutants removal by Sono-photo-Fenton processes. *J. Environ. Chem. Eng.* **2020**, 8, 104330.
29. Giwa, A.R.A.; Bello, I.A.; Olabintan, A.B.; Bello, O.S.; Saleh, T.A. Kinetic and thermodynamic studies of fenton oxidative decolorization of methylene blue. *Heliyon* **2020**, 6, e04454.
30. Khelifi, S.; Ayari, F. Modified bentonite for anionic dye removal from aqueous solutions. Adsorbent regeneration by the photo-Fenton process. *Comptes Rendus Chim.* **2019**, 22, 154–160.
31. Galeano, L.A.; Guerrero-Flórez, M.; Sánchez, C.A.; Gil, A.; Vicente, M.Á. Disinfection by chemical oxidation methods in: Gil, A.; Galeano, L.; Vicente, M. (Eds.) Applications of Advanced Oxidation Processes (AOPs) in Drinking Water Treatment. *The Handbook of Environmental Chemistry*: Springer, Cham; **2017**; p 257.
32. Sun, S.P.; Guo, H.Q.; Ke, Q.; Sun, J.H.; Shi, S.H.; Zhang, M.L.; Zhou, Q. Degradation of antibiotic ciprofloxacin hydrochloride by photo-fenton oxidation process. *Environ. Eng. Sci.* **2009**, 26, 753–759.
33. Sohrabi, M.R.; Khavaran, A.; Shariati, S.; Shariati, S. Removal of Carmoisine edible dye by Fenton and photo Fenton processes using Taguchi orthogonal array design. *Arab. J. Chem.* **2017**, 10, S3523–S3531.
34. Lucas, M.S.; Peres, J.A. Decolorization of the azo dye Reactive Black 5 by Fenton and photo-Fenton oxidation. *Dye. Pigment* **2006**, 71, 236–244.
35. Gou, Y.; Chen, P.; Yang, L.; Li, S.; Peng, L.; Song, S.; Xu, Y. Degradation of fluoroquinolones in homogeneous and heterogeneous photo-Fenton processes: A review. *Chemosphere* **2021**, 270, 129481.
36. Behnajady, M.A.; Modirshahla, N.; Ghanbary, F. A kinetic model for the decolorization of C.I. Acid Yellow 23 by Fenton process. *J. Hazard. Mater.* **2007**, 148, 98–102.
37. Yu, H.; Liu, Y.; Xu, M.; Cong, S.; Liu, M.; Zou, D. Hydroxylamine facilitated heterogeneous fenton-like reaction by nano micro-electrolysis material for rhodamine B degradation. *J. Clean. Prod.* **2021**, 316, 128136.
38. Jain, R.; Mendiratta, S.; Kumar, L.; Srivastava, A. Green synthesis of iron nanoparticles using *Artocarpus heterophyllus* peel extract and their application as a heterogeneous Fenton-like catalyst for the degradation of Fuchsin Basic dye. *Curr. Res. Green Sustain. Chem.* **2021**, 4, 100086.
39. Lin, J.; Wang, L. Comparison between linear and non-linear forms of pseudo-first-order and pseudo-second-order adsorption kinetic models for the removal of methylene blue by activated carbon. *Front. Environ. Sci. Eng. China.* **2009**, 3, 320–324.

40. Simonin, J.P. On the comparison of pseudo-first order and pseudo-second order rate laws in the modeling of adsorption kinetics. *Chem. Eng. J.* **2016**, 300, 254–263.
41. Tran, H.N.; You, S.J.; Hosseini-Bandegharaei, A.; Chao, H.P. Mistakes and inconsistencies regarding adsorption of contaminants from aqueous solutions: A critical review. *Water Res.* **2017**, 120, 88–116.
42. Ulu, H.B.; Değermenci, N.; Dilek, F.B. Removal of chloridazon pesticide from waters by Fenton and photo-Fenton processes. *Desalin. Water Treat.* **2019**, 194, 426–438.
43. Çalık, Ç.; Çifçi, D.I. Comparison of kinetics and costs of Fenton and photo-Fenton processes used for the treatment of a textile industry wastewater. *J. Environ. Manage.* **2022**, 304, 114234.